POAC'17
Busan, KOREA

Proceedings of the 24th International Conference on
Port and Ocean Engineering under Arctic Conditions
June 11-16, 2017, Busan, Korea

Global Ice Load Prediction for the Icebreaker Using 6-DOF Motion Measurement Method

Sang Chul Lee[1], Sunho Park[1], Kyungsik Choi[1], and Seong-Yeob Jeong[2]
[1] Korea Maritime and Ocean University, Busan, Korea
[2] Korea Research Institute of Ships and Ocean Engineering, Daejeon, Korea

ABSTRACT

A global ice load acting on a hull of an icebreaker with a six degrees of freedom (6-DOF) inertial measurement system method was described in this paper. The 6-DOF inertial measurement system treat the ship as a rigid body and measures whole ship motions, and the global ice loads were calculated with the data measured by full-scale ice sea trials of Korean ice breaking research vessel (IBRV) ARAON during her voyage in 2015. To calculate the maximum global ice load, the point of impact (POI) approach and the center of gravity (COG) approach were used, respectively. The differences of the calculated results using the POI and COG approaches were from 254% to 1,794%. Comparing with the resultant forces from strain gauges which ranged from 0.11 to 0.8 MN, the global ice loads from the POI approach were from 59% lower to 239% higher than forces from the strain gauges, and the global ice loads from the COG approach were up to 1,907% higher than the forces from the strain gauges. The calculated global ice loads from both the POI and COG approaches were within the range of an empirical ice load estimation formula under normal operating conditions.

KEY WORDS: Korean IBRV ARAON; Global ice load; 6-DOF motion measurement method; COG approach; POI approach.

INTRODUCTION

Exact ice load estimation is very important for icebreakers that operate in the ice seas. This is because fundamental design factors, such as a hull structure, hull form, and thruster type, are determined based on it.

To measure the global ice loads acting on the hull of an icebreaker, strain gauges were used traditionally. In this method, the hull of an icebreaker is treated as an elastically deformable body, and the ice load is measured by the deformation of the hull during it interacts with the sea ice. Although this method has been proved as an effective and a reliable method, it needs much time and cost for installation and operation. In addition, every time when it is applied

on another hull, same amount of time and cost have to be spent repeatedly.

Then another method which uses the inertial measurement system named as MOTAN (MOTion-ANalysis) was introduced by the Canadian Hydraulic Centre (CHC) of the National Research Council of Canada (Johnston et al., 2003). In this method, the hull of an icebreaker is treated as a rigid body, and the global ice load is measured by the whole-ship motions in the six-degrees of freedom. It is economical for installation and operation, and simple for applying on another icebreaker to predict the global ice loads on a hull.

In this study, global ice loads on the Korean ice breaking research vessel (IBRV) ARAON was predicted using the data measured by an inertial measurement system during her Arctic Ocean voyage in 2015. This Arctic Ocean voyage allocation was carried out from July 30 to August 23, 2015 in the Chukchi and East Siberian Seas.

The motion data in six-degrees of freedom were measured by an inertial measurement system "MotionPak Ⅱ" of SYSTRON DONNER INERTIAL, Inc., which shown in Figure 1, and it consists of three translational accelerometers and three angular rate sensors then each sensor measures the total ship accelerations and the angular rotational rates of the ship in the directions of x-, y-, and z-coordinates, respectively.

Figure 1. Inertial measurement system "MotionPak Ⅱ" of SYSTRON DONNER INERTIAL, Inc.,

DATA PROCESS

Data Calibration and Filtering

For calculating the global ice loads using the measured raw data from the inertial measurement system, two-stepped data processing procedures are required. The first step is data calibration. Since there is no six-degrees of freedom motion before the ice breaker collides with the sea ice, so all the initial values of the raw data have to be shifted to the base level, i.e., set to zero. The second step is data filtering with a low pass filter (LPF). Since the raw data of the inertial measurement system contain motions that are related with modal vibrations and not with sea ice interactions, those motions have to be removed by filtering. It was well known that whole-ship motions commonly occur at the lower frequencies than 5 Hz,

and the higher frequencies than 2 Hz are related with the secondary ship vibrations that are quite separated from the global ship accelerations. Therefore the frequencies higher than 2 Hz must be removed (Chen et al., 1990; Johnston et al., 2004).

As the results after the calibration and filtering procedures, the comparison of acceleration in the y-direction between the raw and processed data was shown in Figure 2, and it was found that the amplitude of the processed data becomes smaller than the raw data because the components of the higher frequencies were removed. Also, The result of the analysis of signal intensity using the fast Fourier transform (FFT) shows that the signals of the higher frequencies than 2 Hz were attenuated rapidly, as shown in Figure 3, by the effect of the filter.

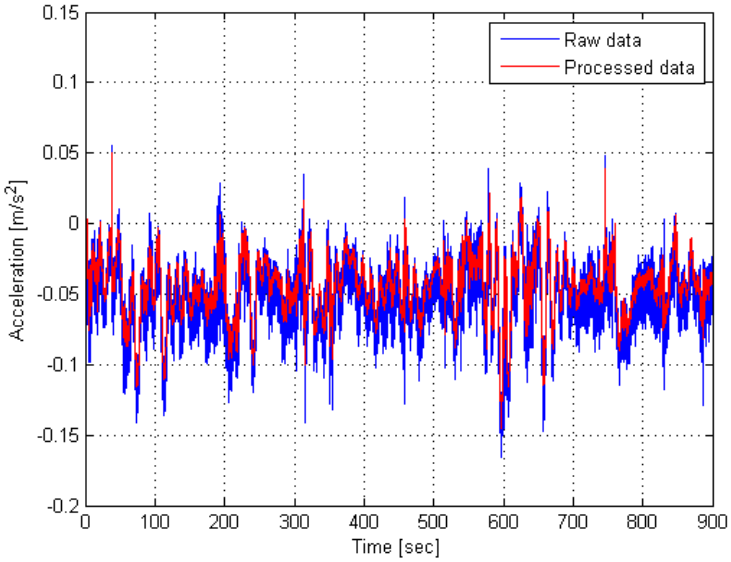

Figure 2. Comparison of amplitudes between raw and processed accelerations in y-direction

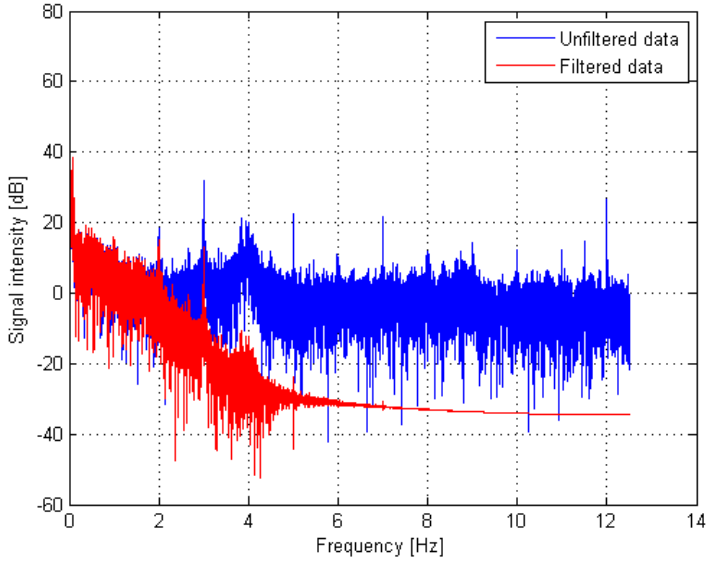

Figure 3. Comparison of signal intensities between unfiltered and filtered accelerations in y-direction

Numerical Calculation

For convenience, the subscripts 1, 2, and 3 represent the translational components of x-, y-, and z-coordinate axes, and the subscripts 4, 5, and 6 represent the rotational components of x-, y-, and z-coordinate axes, respectively. The capital letters *A*, *V*, and *D* represent the acceleration, velocity (or rate), and displacement, respectively. When using above notations, consequently, all measured variables by the inertial measurement system are A_1, A_2, A_3, V_4, V_5, and V_6.

The unknown angular accelerations A_4, A_5, and A_6 were calculated by the numerical differentiation using the known angular rates V_4, V_5, and V_6, respectively, and the numerical differentiation can be written

$$f'(t) = \{f(t + \Delta t) - f(t)\}/h \tag{1}$$

where *t* is time, and Δt is measuring time step.

The other unknown variables were calculated by the numerical integration, i.e., V_1, V_2, and V_3 were from A_1, A_2, and A_3.. The trapezoidal rule was used for the numerical integration (Atkinson, 1993), and it can be written as

$$\int_{t_o}^{t_o+\Delta t} f(t)dt = \Delta t[\{f(t_o + \Delta t) + f(t_o)\}/2] \tag{2}$$

The relations between the variables, and numerical differentiation and integration are shown in Figure 4.

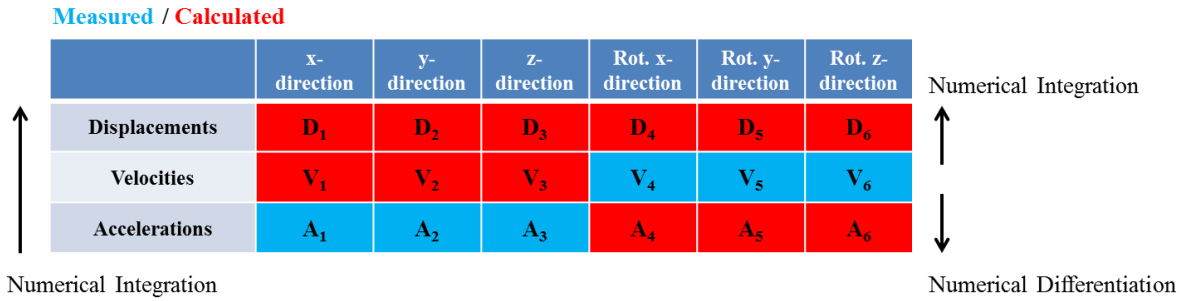

Figure 4. Relations between variables and numerical methods

GLOBAL ICE LOAD

Equations of Motion and Coefficients

The external forces and moments which will be used to calculate the global ice loads can be obtained by the equations of motion in six-degrees of freedom, and the equations of motion can be written as

$$\left[M_{ij} + M_{a_{ij}}\right]\{A_j\} + [B_{ij}]\{V_j\} + [C_{ij}]\{D_j\} = \{F_i\} \quad (3)$$

where M_{ij} is the mass matrix, M_{aij} is the added mass matrix, B_{ij} is the damping coefficient matrix, C_{ij} is the restoring coefficient matrix, A_j is the acceleration vector, V_j is the velocity vector, D_j is the displacement vector, and F_i is the external force and moment vector. The coefficient matrices such as the mass, added mass, and restoring coefficient were calculated using the potential flow-based simulation code.

Global Ice Load Calculations

The external forces and moments obtained by the equations of motion were generated by the interactions between the ship and the sea ice, and they are acting on the center of gravity. F_1, F_2, and F_3 means the external forces acting on the center of gravity in the directions of x-, y-, and z-coordinate axes, i.e., surge, sway, and heave forces, and F_4, F_5, and F_6 means the external moments acting on the same position in the rotational directions about x-, y-,and z-coordinate axes, i.e., roll, pitch, and yaw moments, respectively.

To calculate the maximum global ice load, two approaches, i.e., the point of impact (POI) approach that can be used when the location of impact with ices is exactly known and while the center of gravity (COG) approach that can be used when the impact location is not known, were used, respectively (Johnston et al., 2008a; Johnston et al., 2008b).

For the COG approach, the global ice load was calculated at the center of gravity, and the surge, sway, and heave forces acting on the center of gravity were used. The resultant global ice load is calculated as

$$F_{COG} = \sqrt{(F_1)^2 + (F_2)^2 + (F_3)^2} \quad (4)$$

where F_1, F_2, and F_3 are the surge, sway, and heave forces acting on the center of gravity, respectively.

For the POI approach, the global ice load was calculated at the point of impact, and this approach can be used only when the exact ice impact locations are known. In this approach, the surge force, and yaw and pitch moments acting on the center of gravity were used, and the resultant global ice load is calculated as

$$F_{POI} = \sqrt{(F_1)^2 + (F_6/X_{ab})^2 + (F_5/X_{ab})^2} \quad (5)$$

where F_6 and F_5 are the yaw and pitch moments acting on the center of gravity, and X_{ab} is the longitudinal distance in the direction of x-coordinate axis from the location where the inertial measurement system is installed to the point of impact.

RESULTS AND DISCUSSION

Motion Data Analysis

The translational accelerations and rotational angular rates measured by the inertial measurement system were shown in Figures 5 and 6. In the general icebreaking process with the level ice, the surge motions which appear during the ship collides with the ice and the pitch motions which appear in the process of ice breaking that the ice breaker glides over the ice and crushes it downward with her weight are dominant. However, in the data of year 2015, the sway motions in the translational accelerations, and the roll and yaw motions in the angular rates are dominant as shown in Figures 5 and 6. This is because the ice conditions during the Arctic Ocean voyage in 2015 were not the level ice but small pack ices.

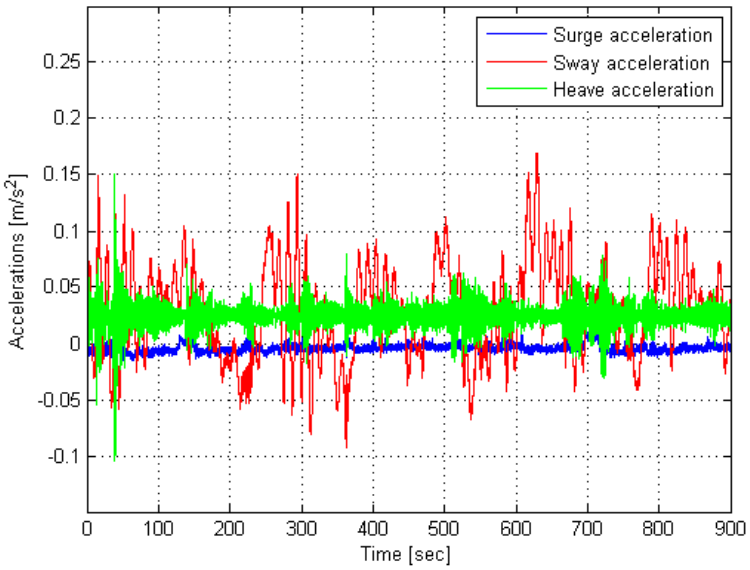

Figure 5. Translational accelerations measured by inertial measurement system

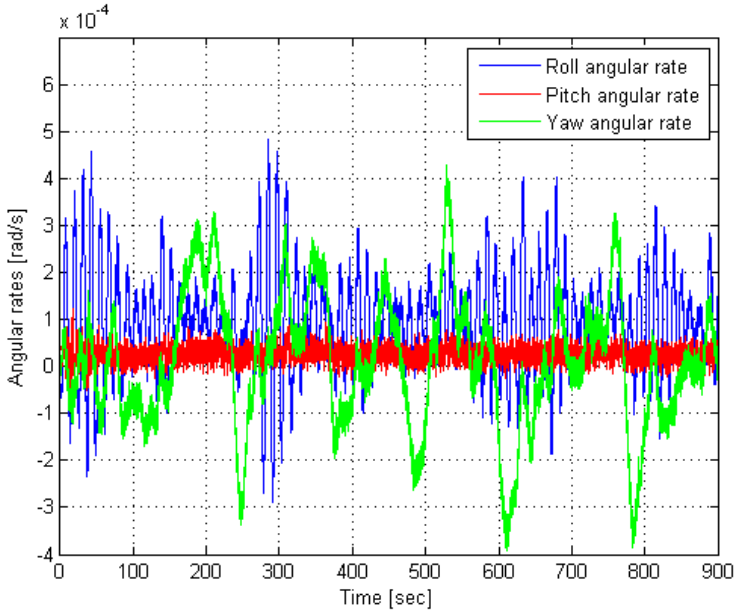

Figure 6. Angular rates measured by inertial measurement system

Global Ice Loads

The global ice load calculations were performed for the total of 138 tests in 30 cases. The resultant global ice loads ranged from 0.11 to 1.06 MN using the POI approach and from 1.41 to 4.87 MN using the COG approach, respectively. At this time, the ship speed corresponding to each test was calculated by using a global positioning system (GPS) device information and the range was from 0.3 to 7.4 *m/s*. The maximum deviation between the POI and COG approaches was 1,794% for the case of the Official 26_2, i.e., the second test in the 26th official case, and the minimum one was 254% for the case of the Official 28_1. The global ice loads for the cases of Official 26-2 and 28_1 were shown in Figures 7 and 8.

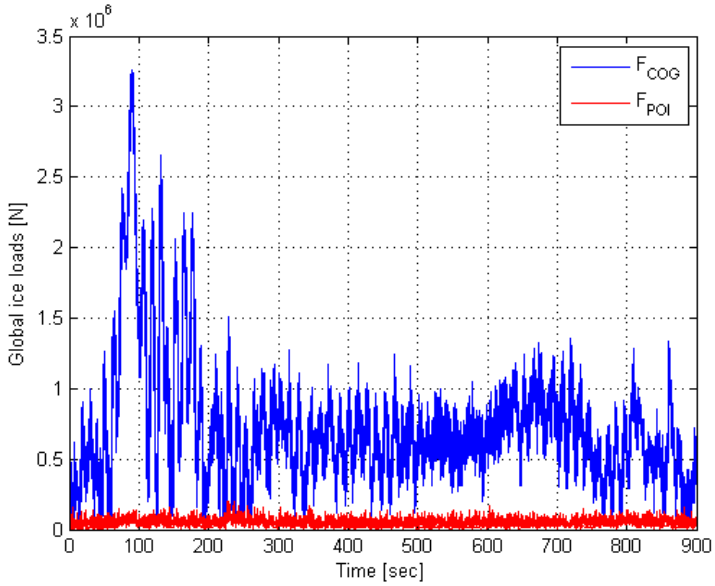

Figure 7. Global ice loads for case of Official 26_2

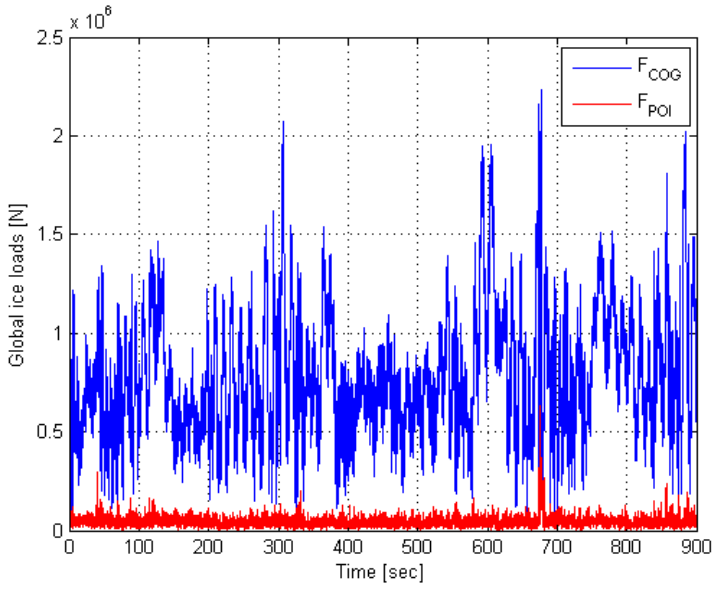

Figure 8. Global ice loads for case of Official 28_1

Comparison with Results of Strain Gauges

The resultant global ice loads calculated from the inertial measurement system were compared with the forces measured from the strain gauge (Min et al., 2016) for the cases of the Official 5, 14, 19, 23, and 28 that contain four tests in each case, and the results were shown in from Figures 9 to 13. The ice loads calculated from the COG approach were consistently much higher than those of the strain gauges, but the ice loads from the POI approach were lower or higher than those of the strain gauges and showed the better agreement with the result of the strain gauges. On the other hand, when considering the ship speed, there is no clear relationship between the ship speed and the ice load. It seems that the weight of each pack ice was more important to generate ice loads than the ship speed.

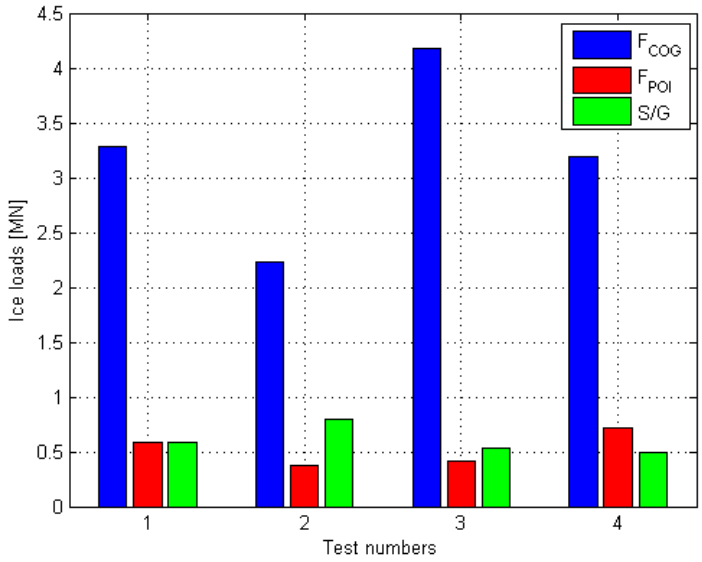

Figure 9. Resultant ice loads from COG and POI approaches and strain gauge for the case of Official 5

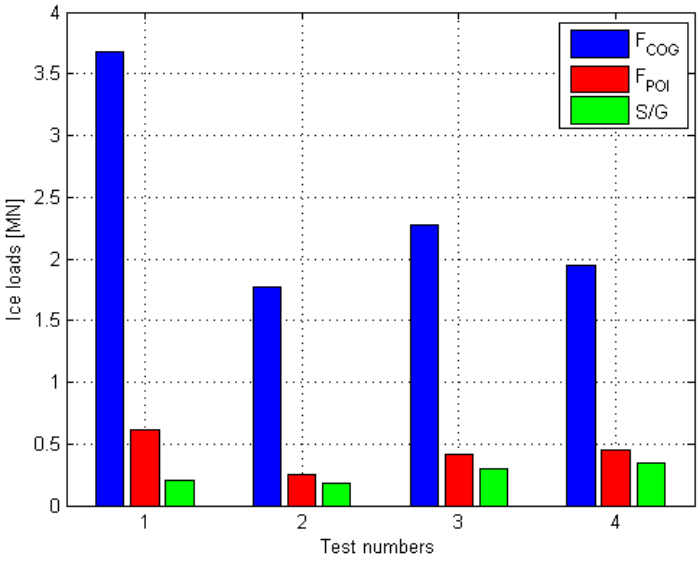

Figure 10. Resultant ice loads from COG and POI approaches and strain gauge for the case of Official 14

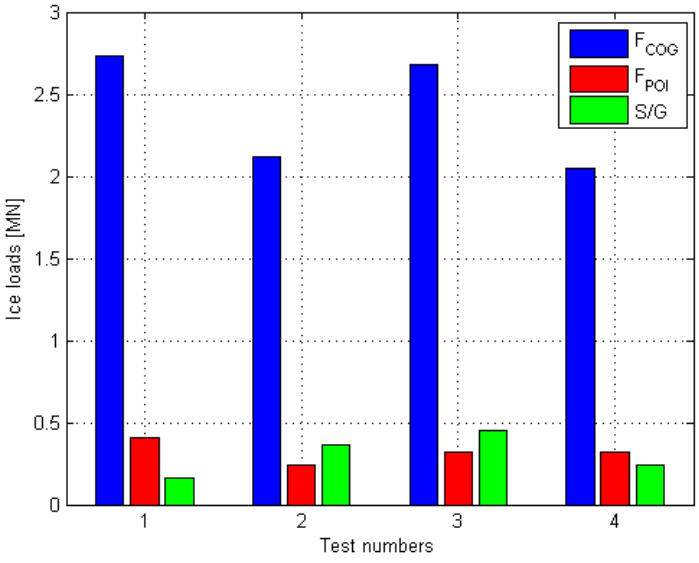

Figure 11. Resultant ice loads from COG and POI approaches and strain gauge for the case of Official 19

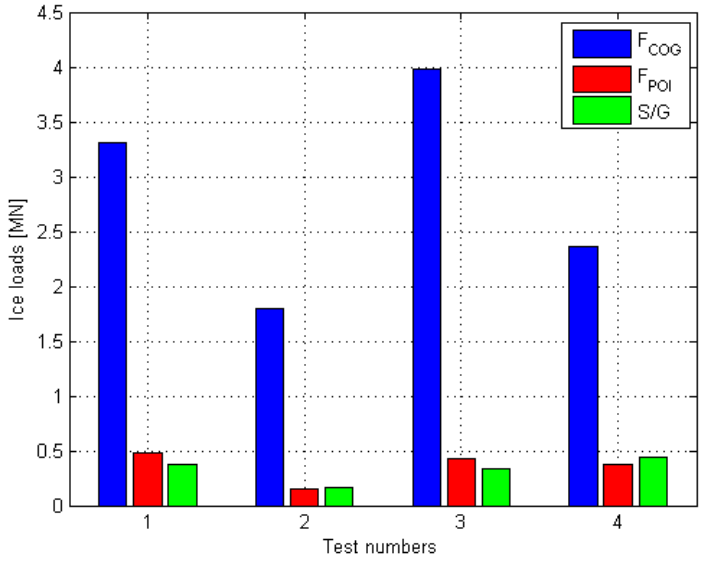

Figure 12. Resultant ice loads from COG and POI approaches and strain gauge for the case of Official 23

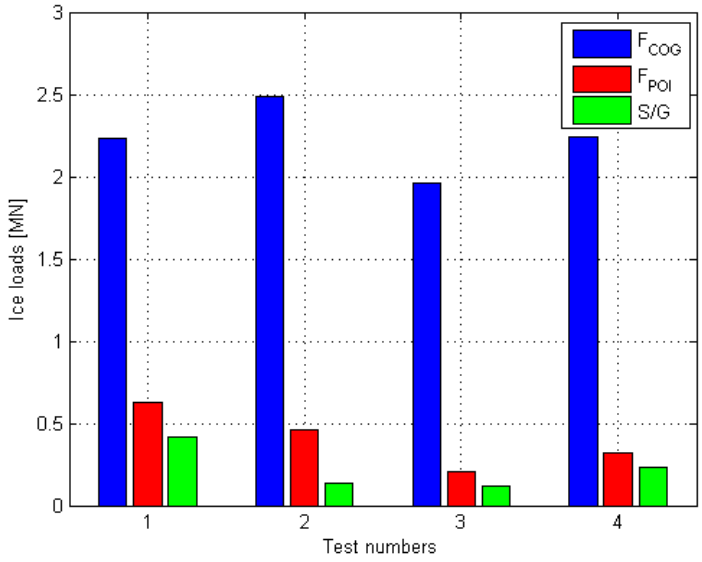

Figure 13. Resultant ice loads from COG and POI approaches and strain gauge for the case of Official 28

Comparison with the Empirical Ice Load Formula

The resultant global ice loads calculated from the inertial measurement system were compared with the empirical ice load estimation formula under the normal operating conditions (Choi et al., 2009) and the formula is expressed as

$$F = 0.824\,\Delta^{0.4}\left(\sigma_f\, h^2\, V\, \cos\alpha\right)^{0.283} \quad (6)$$

where Δ (10^3ton) is the displacement of a ship, σ_f (kPa) is the flexural strength of ice, h (m) is the ice thickness, V (m/s) is the ship speed, and α (degree) is the stem angle of ship. The values of 1 m and 315 kPa were used for the ice thickness and the flexural strength of ice.

The comparison of the calculated ice loads from the inertial measurement system and the strain gauge for the eight cases in the previous section with the estimated ice loads under the normal operating conditions was shown in Figure 14. All the calculated ice loads located below the ice loads estimation formula curve hence they were within the range of the empirical ice load estimation formula under the normal operating conditions. Additionally, all the calculated ice loads showed much lower values than the estimation formula, and there might be several reasons for this. The estimation ice load formula is derived from the conditions with a continuous icebreaking of the level ice with the same material properties, such as the thickness and the flexural strength, while the ice conditions in 2015 were small pack ices. And since the small pack ices are not fixed at one end like a cantilever, the actual flexural strength was considered to be much smaller than the value of 315 kPa used in the calculation. Finally, when the video taken during the voyage in 2015 was investigated (Min et al., 2016), it was estimated that the thickness of the actual sea ice is thinner than 1 m used in the calculation.

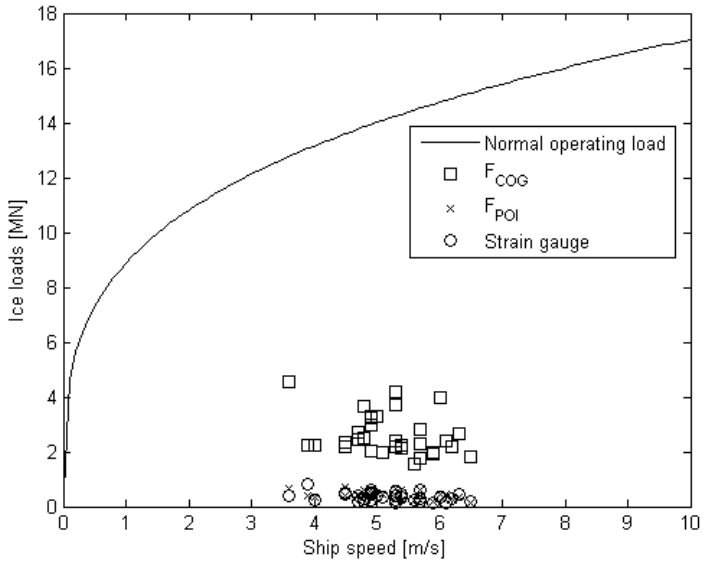

Figure 14. Comparison of calculated ice loads with the empirical ice load estimation formula under normal operating conditions

CONCLUSIONS

To solve the equations of motion, and calculating the global ice loads, procedures, such as calibration, filtering, numerical differentiation and integration were presented. The global ice loads were calculated with the assumption that the ship hull is the rigid body from the motion data. The center of gravity (COG) approach and the point of impact (POI) approach were used to calculate the global ice loads, respectively. From the motion data, the sway, roll and yaw motions were dominant in the collision with the small pack ices because the pack ices were pushed to the side. The ice loads from the COG approach was calculated larger than the

those from the POI approach. The ice loads from the strain gauges was similar to those from the POI approach. On the other hand, when considering the ship speed, there is no clear relationship between the ship speed and the ice load.

All the calculated ice loads were within the range of the empirical ice load estimation formula under the normal operating conditions, but their values were very small compared to the estimation formula. This is due to the fact that the ice conditions were small pack ices, whereas the estimation formula is originally to estimate of the ice load for continuous icebreaking in level ice.

ACKNOWLEDGEMENTS

Our research was supported by the National Research Foundation (2015037577) and the IT R&D Program of MOTIE/KEIT (10060329) funded by the Korea government, and carried out within the scope of the primary program ("Establishment of experimental foundation for unconventional test to evaluate hydrodynamic performance of ships," Project No. PES3550), which is funded by KRISO.

REFERENCES

Atkinson, K., 1993. Elementary Numerical Analysis. John Wiley & Sons, pp.161-204.

Butterworth, S., 1930. On the theory of filter amplifier. Experimental Wireless & the Wireless Engineer, 7, pp.536-541.

Chen, Y., Tunik, A., & Chen, A., 1990. Global Ice Forces and Ship Response to Ice – Analysis of Ice Ramming Forces. Report submitted to Maritime Administration by American Bureau of Shipping, Report SSC-342, pp.104.

Choi, K., Jeong, S.Y., & Nam, J.H., 2009. Prediction of Design Ice Load on Icebreaking Vessels under Normal Operating Conditions, Proceedings of the 20th Int Conf on Port and Ocean Engineering under Arctic Conditions, Lulea, Sweden, 9-12 June, 2009.

Johnston, M., Frederking, R., Timco, G., & Miles, M., 2003. MOTAN: A Novel Approach for Determining Ice-induced Global Loads on Ships, Proceedings of MARI-TECH 2003, Montreal, Canada, 28-30 May, 2003.

Johnston, M., Frederking, R., and Timco, G., and Miles, M., 2004. Using MOTAN to Measure Global Accelerations of the CCGS Terry Fox During Bergy Bit Trials, Proceedings of 23rd Int Conf on Offshore Mechanics and Arctic Engineering, Vancouver, Canada, 20-25 June, 2004.

Johnston, M., Ritch, R., & Gagnon, R., 2008a. Comparison of Impact Forces Measured by Different Instrumentation systems on the CCGS Terry Fox During the Bergy Bit Trials. Cold Regions Science and Technology, 52, pp83-97.

Johnston, M., Timco, G., Frederking, R., and Miles, M., 2008b. Measuring Global Impact Forces on the CCGS Terry Fox with an Inertial Measurement System Called MOTAN. Cold Regions Science and Technology, 52, pp67-82.

Min, J.K., Cheon, E.J., Kim, J.M., Lee, S.C., & Choi, K., 2016. Comparison of the 6-DOF Motion Sensor and Strain Gauge Data for Ice Load Estimation on IBRV ARAON. Journal of the Society of Naval Architects of Korea, 53(6), pp.529-535.

Newman, J.N., 1997. Marine Hydrodynamics. The MIT Press, pp.295-300.

Salvesen, M., Tuch, E.O., & Faltinsen, O., 1970. Ship Motions and Sea Loads. Transactions of Society of Naval Architects and Marine Engineers, 78, pp.250-287.

Timco, G., & O.'Brien, S., 1994. Flexural Strength Equation for Sea Ice. Cold Regions Science and Technology, 22(3), pp.285-298.